19

Using Monte Carlo Method to Study Magnetic Properties of Frozen Ferrofluid

Tran Nguyen Lan and Tran Hoang Hai
HoChiMinh City Institute of Physics,
Vietnamese Academic of Science and Technology
Viet Nam

1. Introduction

Magnetic nanoparticles are single-domain particles of ferromagnetic or ferrite materials. Recently, magnetic nanoparticles have been applied more and more in technology, such as spintronics, magnetic recording, catalyst, and biomedicine. Therefore, experimental and theoretical studies on their magnetic properties are very important to provide essential information for individual applications. In addition, technical preparations have been developed fast, such as chemical synthesis, sputtering, or lithography. Depending on characters of assemblies, magnetic properties are different, such as two- or three-dimension, metallic or metallic oxide materials, order or disorder arrangement, surrounded by solids (granular solids) or liquids (ferrolfuids), and the magnetic or non-magnetic surrounding matrix. This leads to studying fundamental properties of magnetic nanoparticle assemblies becomes interesting.

Among applicable potentials of magnetic nanoparticles, the biomedicine is a promising area, because the magnetic nanoparticles offer some great possibilities (Pankhurst et al., 2003). First, their size ranges from a few nanometers up to tens of nanometers. This means that their size can be smaller than of comparable to the size of biological entities, for example, a cell (10 – 100 μm), a virus (20 – 450 nm), a protein (5 – 50 nm) or a gene (2 nm wide and 10 – 100 nm long). Thus, they can penetrate easily into these entities. Second, these particles behave magnetic properties, so they can be controlled by an external magnetic field gradient. This opens application including the transport (drug delivery, cell separation) or immobilization (hyperthermia, contrast agent). Third, these particles can strongly resonate to a radio field. This makes them be easily excited by radio field leading, for example, heating in hyperthermia or magnetic resonance in contrast agent.

A key quality to study magnetic properties of particle is magnetic anisotropy energy (MAE). However, it is very difficult to exactly observe the MAE of each particle in the assembly. We can just obtain the MAE distribution of the assembly. Usually, the MAE distribution $f(E_B)$ is deduced from the size distribution f(V) due to simplest expression of MAE, $E_B = KV$, with K and V as anisotropy constant and volume, respectively, of each particle. However, this way does not describe the exact information of real systems. It is due to some reasons as follow. (i) The size distribution obtains from microscopy images may not coincide with the real sample. (ii) The magnetic anisotropy involves many complexities, such as surface, magneto-

crystal, or shape. (iii) The orientation of anisotropy axis of particles in the assemblies is random, thus this way can not give the precise response between the size and the energy barrier distribution. A recent review written by Zheng et al. (Zheng et al., 2009) showed that there are some different ways to extract the anisotropy distribution, however, for the dilute sample. The problem becomes much more complex as the inter-particle interactions arise, namely dipolar interaction (for example, Bottoni et al., 1993; Ceylan et al, 2005; Parker et al., 2008) exchange interaction due to the contact between surface of particles or the magnetic surrounding matrix (for recent example, Tamion et al., 2010; Malik et al., 2010). However, the numerical analyses or phenomenal theory has not provided sufficient explanations for the observations of experiments. Therefore, computer simulations, especially Monte Carlo simulation, become efficient.

Now, to clearly see the successes of the Monte Carlo (MC) simulation of magnetic nanoparticle assemblies, we will shortly list some the important results. Kechrakos & Trohidou (Kechrakos & Trohidou, 1998) employed the MC simulation to give a general view about the interacting assemblies. Following these results, interacting assemblies possesses the anti-ferromagnetic state (decrease of magnetic responses) and ferromagnetic state (increase of magnetic responses) at low and high temperature, respectively. At the same time, MC method was used to seek the spin-glass (SG) like behavior of interacting systems at the low temperature. While almost results show the SG like behavior (for example, Anderson et al., 1997; Ulrich et al., 2003; Iglesias and Labarta, 2004; Fernadez and Aloso, 2009; …), a few other results opposed the presence of SG like behavior (Garcia-Otero et al., 2000; Porto, 2005). Recent results based on the combination between the magnetic force microscopy and the MC simulation proved the existence of the short-range magnetic order deduced by dipolar interaction at the high temperature (Georgescu et al., 2006, 2008). These results visually asserted the role enhancing the energy barrier of anisotropic character along the bond axes of dipolar interaction. In addition, MC simulation is also a cost tool to investigate the structure of particle-cluster in assemblies (for a most recent example, Prokopieva et al., 2009). In this chapter, we will review some our recent results on magnetic properties of frozen ferrofluids.

Our chapter is organized as follow. In the part 2, we present two models describing the magnetic properties of dilute sample and the interacting sample. Therefore, we can see the limitation of these phenomenal models. In the third part, there are three section are presented, the field dependence of the blocking temperature, the concentration dependence of the coercive field, and the effective anisotropy distribution deduced by dipolar interaction. These results are clearly explained and compared to found experiments. Finally, we provide a short conclusion as well as some future aspects.

2. Some phenomenal models

2.1 Neel - Brown model

We first discuss the Neel – Brown (NB) model (Neel, 1953; Brown, 1963) which is used to describe the magnetic properties of assemblies in the non-interacting case. In this model, the relaxation of each particle moment in the assemblies depends on the competition between the thermal fluctuation k_BT and the barrier energy E_B, which defined by the magnetic anisotropy of each particle. First assumption of this model is that each particle moment is formed by the rigid alignment of atomic spins; therefore, the reversal of particle moments is

the coherent rotation of atomic spins. The relaxation time, without external field, is characterized by the Arrhenius law as follow

$$\tau = \tau_0 \exp\left(\frac{E_B}{k_B T}\right) \tag{1}$$

Where τ is relaxation time and τ_0 is characteristic time which is a function of gyro-magnetic ratio, longitudinal magneto-striction constant, and Young modulus. Neel estimated τ_0 to be of order 10^{-10} s, this value is good agreement with experiments. Following the expression (1), if $k_BT << E_B$ the τ is so large (very slow relaxation) that relaxation can not be observed, that is the assembly seems to be an ordered magnetic system. On the contrary, if $k_BT >> E_B$ the relaxation is very fast, so the assembly reach to the thermal dynamic equilibrium. Therefore, there is a finite temperature which separates two above regimes. This temperature is called the blocking temperature and determined from the expression (1)

$$T_B = \frac{E_B}{k_B \ln\left(\tau_m / \tau_0\right)} \tag{2}$$

with τ_m as the measured time-window. Clearly that T_B strongly depends on the τ_m which is defined by experimental conditions, so the blocking temperature is not unique.
For $T < T_B$, magnetic moments can not reverse and the assembly is in the blocking state exhibiting hysteresis. For $T > T_B$, the magnetic moments easily reverse, the hysteresis disappears and the assembly is in the super-paramagnetic states (SPM). In the case of uniaxial anisotropy barrier with anisotropy constant as K_u, $E_B = K_uV$, the blocking temperature has form

$$T_B = \frac{K_u V}{k_B \ln\left(\tau_m / \tau_0\right)} \tag{3}$$

In the poly-dispersity sample, the blocking temperature of sample is an average of all blocking temperatures of individual particles. Namely

$$\langle T_B \rangle = \frac{\int T_B(V) f(V) dV}{\int f(V) dV} \tag{4}$$

with $<T_B>$ as the blocking temperature of sample.
In the presence of the external field, the anisotropy barrier is reduced, $E_B = K_uV(1 - H/H_a)^{\alpha}$, with $H_a = 2K_u/M_s$ as the anisotropy field, M_s as saturated magnetization and the parameter α closes to 1.5 (Knobel et al., 2008) or 2 (Kechrakos, 2010). The blocking temperature of each particle has form

$$T_B = \frac{K_u V}{k_B \ln\left(\tau_m / \tau_0\right)}\left[1 - \frac{H}{H_a}\right]^a \tag{5}$$

with $T_B(0)$ as the blocking temperature of each particle in the absence of external field. Following the expression (5), the blocking temperature would monotonic decrease with

increasing the external field. However, the experimental results showed a non-monotonic field dependence of blocking temperature in the dilute sample. We will explain this contrary by Monte Carlo simulation in the fourth part. Effect of inter-particles interactions on this dependence will be also provided.

2.2 RAM model for interacting particle assemblies

Now, we will briefly consider a recent approach which was developed by Nunes et al. (Nunes et al. 2005). This approach was based on the random anisotropy model (RAM) which was developed to describe the magnetic properties of amorphous magnetic materials. According to RAM model, the correlation length due to interactions between particles is included in the effective value of anisotropy constant K_{eff}. The aim of this approach is to calculate the blocking temperature under the influence of the interactions in the presence of external field. Therefore, the authors began from the expression (5) with the two relevant parameters which need to be modified, namely effective anisotropy and effective volume V_{eff} of particles in the correlation length L (Nunes et al., 2005)

$$K_{eff} = \frac{K}{\sqrt{N}} \text{ and } V_{eff} = \frac{\pi}{6}\left[D^3 - x\left(L^3 - D^3\right)\right] \tag{6}$$

Where N is number of correlated particles and D is the diameter of each particle,

$$N = \left[1 + x\frac{\left(L^3 - D^3\right)}{D^3}\right] \tag{7}$$

As the interaction is weak, L << D, both expressions in (6) will tend to the anisotropy and volume of individual particles.

Next, the authors gave the correlation length as a function of external field

$$L_H = D + \sqrt{\frac{2A_{eff}}{M_s H_{dc} + C}} \tag{8}$$

with A_{eff} represents the intensity of interactions and C is a parameter to prevent the divergence at zero fields.

By substituting the effective anisotropy and effective volume of each particle in expression (6) on the expression (5), the authors obtained the expression for the blocking temperature of couple particles in the term of structural parameter (Nunes et al., 2005) as follow

$$T_B = \frac{K_u \pi\left[D^3 - x\left({L_H}^3 - D^3\right)\right]}{6k_B \ln\left(\tau_m / \tau_0\right)\left[1 + x\frac{\left({L_H}^3 - D^3\right)}{D^3}\right]^{1/2}}\left\{1 - \frac{H_{dc}}{H_a}\left[1 + x\frac{\left({L_H}^3 - D^3\right)}{D^3}\right]^{1/2}\right\}^a \tag{9}$$

This phenomenal approach obtained several good agreements with experiments of granular solids (Nunes et al., 2005; Knobel et al., 2008). However, it has not still given a general view on collective states of strongly interacting magnetic nanoparticle systems (Knoble et al., 2008).

3. Energy and simulation method

3.1 Energy

In the computer simulation, energy function is an extremely important problem. Therefore, the first work in the computer simulation is to build an energy function which must relate to real systems. Our model is based the earlier studies on Monte Carlo simulation of magnetic nanoparticle systems (for example, Kechrakos and Trohidou, 1998; Garcia-Otero et al., 2000), thus some assumptions are used to introduce the energy as follow

i. Particles possess the totally spherical shape with diameter D. The poly-dispersity of particle size is determined by the log-normal distribution with the width $\sigma < 1$.
ii. The magnetic moment vector of each particle has form $\boldsymbol{\mu} = M_s V\mathbf{e}$. Where M_s, V, and **e** are saturated magnetization, volume, and the unit vector of each magnetic moment, respectively.
iii. Position of particles is randomly arranged in the cubic box of the volume $(n.D)^3$ with n as an integer.
iv. The anisotropy of each particle is characterized by uniaxial anisotropy with the anisotropy constant K_u being in the range from 19 $kJ.m^{-3}$ to 190 $kJ.m^{-3}$.
v. Thermal fluctuations of the assembly magnetization are well described by the coherent rotation of magnetic moments of particles.

Basing on the above assumptions, we obtain the total energy function for each particle

$$E^{(i)} = -K_u V_i \left(\frac{\boldsymbol{\mu}_i.\mathbf{n}_i}{|\boldsymbol{\mu}_i|} \right)^2 - \boldsymbol{\mu}_i \mathbf{H} + g\sum_{j\neq i}^{N} \left(\frac{\boldsymbol{\mu}_i.\boldsymbol{\mu}_j}{r_{ij}^3} - 3\frac{\left(\boldsymbol{\mu}_i.\mathbf{r}_{ij}\right)\left(\boldsymbol{\mu}_j.\mathbf{r}_{ij}\right)}{r_{ij}^5} \right) \tag{10}$$

The first term in Eq.10 is the anisotropy energy, $\mathbf{n}_i$ is the direction of the anisotropy axis, $|\mathbf{n}_i| = 1$. The second term is the Zeeman energy, **H** is the external field. The last time is the dipolar energy between two particles i and j separated by r_{ij}, and constant $g = \mu_0/4\pi$.

Usually, in the mean field theory (Strikmann and Wohlfarth, 1981), the effect of dipolar interaction is represented through the dipolar field which is included into the applied field. However, following the DBS model (Dormann et al., 1999) and some simulated as well as experimental results (for example, Kechrakos and Trohiou, 1998; Verdes et al., 2002; Ceylan et al., 2005; Knobel et al., 2008; …) showed that the dipolar interaction deduces the effect being similar to anisotropy barrier, namely the enhancement of the blocking temperature along with the interacting strength. Therefore, we can include the anisotropic character along bond axes of the dipolar interaction in the anisotropy energy.

1. Case of the inclusion of dipolar field on the applied field, the dipolar field is defined by follow equation

$$\mathbf{H}_{dipol}^{i} = -\sum_{j\neq i}^{N} \frac{\partial U_{dipol}^{ij}}{\partial \boldsymbol{\mu}_i} = -g\sum_{j\neq i}^{N} \left(\frac{\boldsymbol{\mu}_j}{r_{ij}^3} - 3\frac{\mathbf{r}_{ij}.\left(\boldsymbol{\mu}_j.\mathbf{r}_{ij}\right)}{r_{ij}^5} \right) \tag{11}$$

Then, the dipolar energy of the particle i can rewrite in the simple form $U_{dipol}^{i} = \boldsymbol{\mu}_i.\mathbf{H}_{dipol}^{i}$. And the energy of the particle i as

$$E^{(i)} = -K_u V_i \left(\frac{\boldsymbol{\mu}_i.\mathbf{n}_i}{|\boldsymbol{\mu}_i|} \right)^2 - \boldsymbol{\mu}_i \mathbf{H}_i^{eff} \tag{12}$$

Now, the system can be thought as an ensemble of the non-interacting particles feeling an effective field that is sum of an external and a local field $\mathbf{H}_i^{eff} = \mathbf{H} + \mathbf{H}_{dipol}^i$.

2. Case of the inclusion of anisotropic character along bond axes of the dipolar interaction on the uniaxial anisotropy, we rewrite the total energy of each particle

$$E^{(i)} = -K_{eff}^i V_i + gM_S{}^2 \sum_{j \neq i}^{N} \frac{\mathbf{e}_i \mathbf{e}_j}{r_{ij}^3} V_i V_j - M_S V_i \mathbf{e}_i \mathbf{H} \tag{13}$$

The first term in Eq.13 is the effective anisotropy energy with effective anisotropy density

$$K_{eff}^i = K_u \left(\mathbf{e}_i \mathbf{n}_i\right)^2 + 3gM_S{}^2 \sum_{j \neq i}^{N} \frac{\left(\mathbf{e}_i \mathbf{r}_{ij}\right)\left(\mathbf{e}_j \mathbf{r}_{ij}\right)}{r_{ij}^5} V_j \tag{14}$$

The second term in Eq. 13 characterizes the anti-ferromagnetism because of $gM_s^2 > 0$ and it just has significance for N neighbour particles. While the second term in Eq. 14 expresses the ferromagnetic anisotropy along the bond axis. And the effective anisotropy energy of each particle has form

$$E_{Beff}^{(i)} = K_{eff}^i V_i = \left[K_u \left(\mathbf{e}_i \mathbf{n}_i\right)^2 + 3gM_S{}^2 \sum_{j \neq i}^{N} \frac{\left(\mathbf{e}_i \mathbf{r}_{ij}\right)\left(\mathbf{e}_j \mathbf{r}_{ij}\right)}{r_{ij}^5} V_j \right] V_i \tag{15}$$

In our opinion, two above inclusions have different advantages as considering the effect of the dipolar interaction at the different temperature ranges. If the temperature is low, the thermal fluctuation of magnetic moment is very weak. This means that the effect of the dipolar field deduced by a magnetic moment on other moments is very significant. On the other hand, if the temperature is high to make the magnetic moment fluctuate, the dipolar field continuously varied. Therefore, the anisotropic character which enhances the anisotropy barrier becomes more important as we will explain later. In summary, the first inclusion should be used to explain the collective state at the low-temperature and the second one more clearly shows the role enhancing the anisotropy barrier. These inclusions are similar to the mean field theories (Walton, 2007; Dotsenko, 2010) and DBF model (Dormann et al., 1988); however, with computer simulation the interaction field and the effective anisotropy energy are exactly calculated, because their values totally obtain through the configurations of all the moments in the system and they change in each time-step (Kechrakos, 2010). Finally, note that although the applied field was not showed in the Eq.15, its influence is implied through the direction of each magnetic moment.

3.2 Simulation procedure

Monte Carlo method is an easy and fast approach to minimize the energy of random or pseudo-random systems. With the magnetic nanoparticle systems the Metropolis algorithm (Metropolis et al., 1953) is most widely used. Details of this algorithm have been presented in many previous literatures, so in here we just introduce the procedure to obtain the local energy minima of each particle in the assembly. The configurations of magnetic moments are performed in the spherical coordinate. We assume that the external field **H** is applied along the z-axis of the particle system, and easy axis of particles aligned at an angle ψ with the field and the direction of the magnetic moment is determined by values (θ,φ). At the

beginning of each simulation, an assemblage of N particles is generated and random values of φ, and θ are drawn from a uniform distribution $\theta \in [0, 2\pi]$, and $\varphi \in [0, 2\pi]$. The ψ value of each particle is constant throughout the simulations and the variation of φ and θ is of interest. Each Monte Carlo step consists of the following steps

i. Using Eq. (10) the energy of each particle is determined base on the applied field and the current values of θ,φ, this value is E.
ii. A new orientation of the magnetization is selected at random within even angles (dφ and dθ, these values are determined randomly from [-η_{max}, η_{max}]).
iii. The energy E_{trial} is calculated for the particle along with the new values of the magnetization.
iv. The difference ΔE is calculated for the two possible orientations of the magnetization, $\Delta E = E_{trial} - E$.
v. The magnetization of the particle is moved to the new orientation with the probability min [1, exp (-ΔE/K_BT)].

All simulations are performed by the dimensionless parameter of magnetization and applied field viz. m = M/M_S and h = H/H_a, respectively. Following our previous reports (Lan and Hai, 2010), the mean diameter of particles is 7.5 nm.

4. Our results and discussion

4.1 Field dependence of blocking temperature

According to the Neel – Brown model, the blocking temperature will monotonic decrease along with the applied field in the dilute samples. However, many experiments found that this dependence is non-monotonousness with various materials, such as Fe_3O_4, ferritin, γ-Fe_2O_3, Co and FePt (Luo et al., 1991; Friedmann et al., 1997; Sappey et al., 1997; Kachkachi et al., 2000; Zheng et al, 2006). On the contrary, the blocking temperature seems to be invariable at the low-field in the case of dense sample (Kachkachi et al., 2000; Parker et al., 2008). However, there have been no clear explanations by theoretical employment. Therefore, we use the Monte Carlo simulation to investigate these problems.

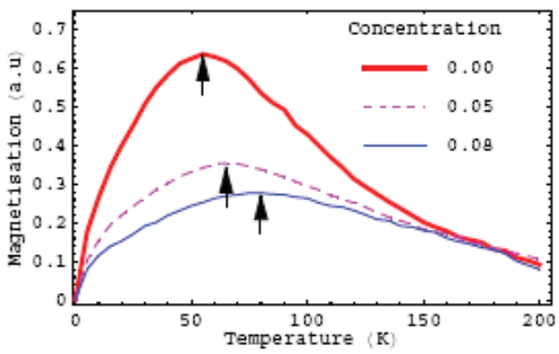

Fig. 1. Temperature dependence of magnetization as a function of concentration, the blocking temperatures (peaks of curves) are shown by arrow (from Lan and Hai 2010)

We define the blocking temperature of assembly as the peak temperature of the zero-field-cooling (ZFC) curve. Therefore, to find the blocking temperature we have to simulate the ZFC process. First the sample is cooled to very low temperature without external field. After that, a small field is applied and the sample is heated up to a very high temperature with the slow rate. The peak of the curve is the blocking temperature. At each the value of

temperature 5.10^4 Monte Carlo steps are used. The results are average of 100 samples with different initial configurations. The energy barrier energy is extracted to explain these results. It is very difficult to build a numerical model that finds the barrier distribution. However, we recognize that the energy difference ΔE in the translation probability is always equal to one of the actual energy barriers of the system (Iglesias & Labarta, 2004). Therefore, we can extract the barrier distribution by using the Monte Carlo method to sample the individual energy barriers of all the particles. Fig. 1 represents the ZFC curve at the different concentration. The peak temperature shifts to the large-value along with the increase of concentration as found in very many previous studies.
Now, we consider the field dependence of the blocking temperature in two cases, dilute and dense sample

4.1.1 Dilute sample

In the Fig. 2a, when the reduced field value is smaller than 0.3, the peak temperature increases along with the increase of the reduced field, and then it continuously decreases along with the increase of the reduced field. The increase of the peak temperature in the low field expresses strongly at the large-σ. As saw in Fig. 2b, the distribution of the energy barrier is sensitive to the applied field, and they are broadened as the field increases at the low values. Sappey et al. (Sappey et al., 1997) suggested that the effect of low fields on the energy barrier distribution could be due to disorder of orientations, or the defects of each particle. Zheng et al. (Zheng et al., 2006) explained that this non-monotonous was due to combining the size distribution and the slow decrease of the magnetization (or non-Curie's law dependence of magnetization) above the blocking temperature in the field.

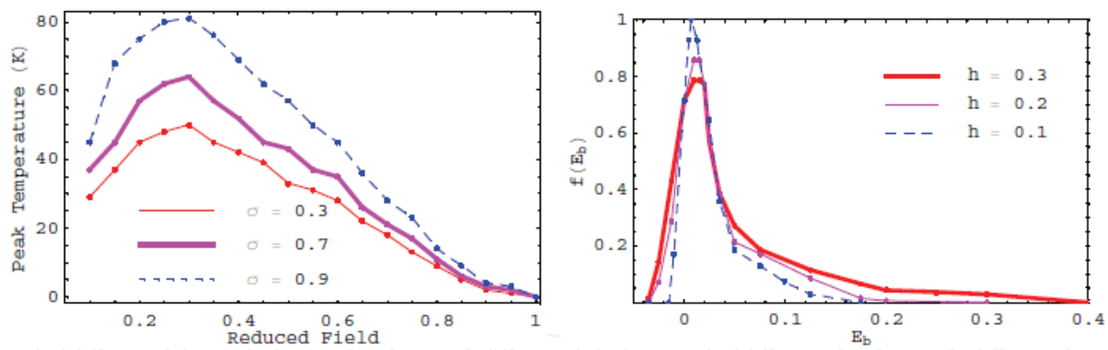

(a) (b)

Fig. 2. a) Field dependence of blocking temperature (peak ZFC curve) and b) the barrier distribution as a function of the low field in the dilute sample (from Lan and Hai 2010)

Although these explanations satisfy with the present model (the unixial anisotropy model), they are simple and not sufficient. Recently, Perez et al. (Perez et al., 2008) showed the effect of the anisotropy ratio (core-shell anisotropy) on the energy barrier distribution of the dilute systems and with increasing the surface anisotropy the energy barrier distribution is enlarged even when the size distribution is quite narrow. Basing on this, we can imagine that under the influence of the low field, the contribution of the surface anisotropy may become dominant in the comparison with the core anisotropy, so the energy barrier distribution of the system is enlarged. At the high field, the Zeeman energy exceeds the anisotropy energy of each particle. Therefore, atomic moments of each particle containing the atomic surface and the atomic core orient along with the field direction, this means that

the disorder at the particle surface disappears. In other words, the contribution of the surface anisotropy is not dominant, so the barrier distribution becomes narrow, and the peak temperature decreases. In our opinion, the non-monotonic behavior of the T_p vs. h curvature expresses strongly in the independent particle systems possessing the strong surface anisotropy. We can use the atomistic simulation methods, such as the first principal calculation, to predict the influence of the applied field on the particle surface structure.

4.1.2 Dense sample

We considered the influence of the dipolar interaction on the behavior of the ZFC-peak vs. applied field curve. A recent numerical study was based on the Gittlmen-Abeles-Bozowski model (Agzegagh & Kachkachi, 2007) to perform the change of the shape of this curve for the weak interaction, but it was complex and at the high concentrations, the numerical analyses are impossible. We need to remember that the dipolar energy of the particle i will make an effective anisotropy which makes the increase the blocking temperature. As we saw in Fig. 3a, the curvature change from the non-monotonousness to monotonousness, and at the very strong interaction, the curvature becomes flatter. As in Fig. 3b, when the interacting strength increases, the relation between the size distribution and the barrier distribution disappears, therefore, the non-monotonousness will change to the monotonousness. However, if the sample is very dense, the dipolar interaction is strong enough to remain the energy barrier at the small values of the applied field. Then the energy barrier of each particle slowly decreases along with the applied field, this means that the curvature is less sloping. Because the strong interaction remain the barrier as mentioned above, the blocking temperature exists even the applied field exceeds the anisotropy field H_a. This scenario also found by Serantes et al. (Serantes et al., 2008), however, the behaviors at the low field are rather different from our results. We find that the curvatures are separated clearly at the low field, because at this region the local field plays dominant role, then the blocking temperature increases along with the increase of the concentration.

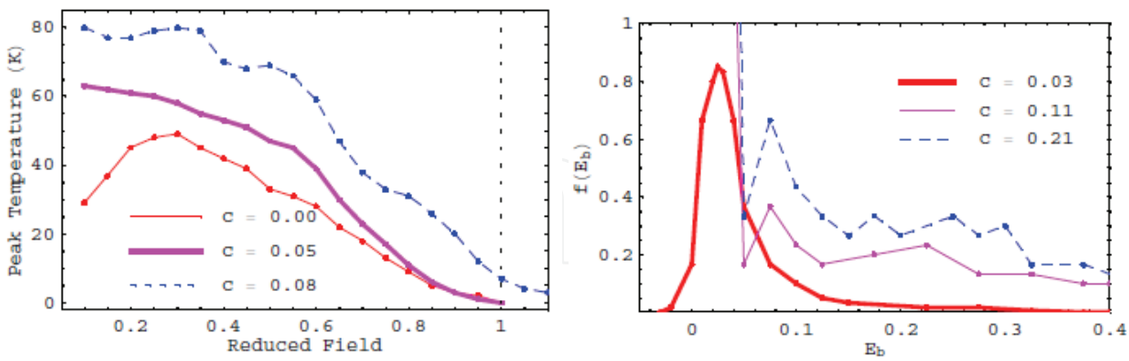

(a) (b)

Fig. 3. a) Field dependence of blocking temperature (peak ZFC curve) and b) the barrier distribution as a function of the low field in the dense sample (from Lan and Hai 2010)

4.2 Concentration dependence of coercive field

Coercive fields are obtained by using the procedure as follow. The sample is first submitted to equilibrium state through 10^4 Monte Carlo steps, and then an external field is applied and

increased until obtaining the saturation of magnetization. The configurations of magnetic moments are recorded and the external field is decreased to zero. The magnetizing process is performed again with the negative direction of the applied field. The coercive field is value at which the magnetization equals to zero. In each increasing (decreasing) step of field 5.10^4 Monte Carlo steps are performed. The results are the average of 100 different samples of random initial configurations. Fig. 4 shows the hysteresis at the temperature T = 10 K as a function of concentration.

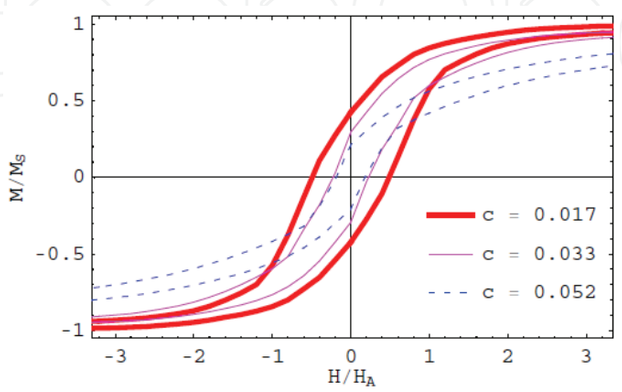

Fig. 4. Hysteresis loops at the low-field as a function of the concentration and the low-temperature is set at 10 K. The results are the average of 100 different samples of random initial configurations (alignment of magnetic moments and arrangement of positions) (from Lan and Hai 2010).

In fact, the concentration dependence of magnetic responses was studied in the previous simulated and experimental works (Bottoni et al., 1993; Kechrakos & Trohidou, 1998; Verdes et al., 2002; Blackwell et al., 2003; Ceylan et al., 2005; Tan et al., 2010). These results found a cusp of the magnetic response vs. concentration curves. However, there are differences in the explanations between the simulations and experiments. Experimental results (Bottoni et al, 1993; Ceylan et al, 2005) asserted that the increase of coercive field along with the concentration is due to the chain-like or small cluster formation which enhances the energy barrier under the influence of interparticle interactions. While the simulation results (Kecrakos and Trohidou, 1998; Verdes et al., 2002) showed that the origin of this cusp is the competition between the blocking and super-paramagnetic states below a concentrated threshold. Although these differences are due to in the real system the particle systematic formations of particle-clusters that do not take place in the simulations, we believe that the magnetic phases are also dominant in the appearance of this cusp. Therefore, to confirm the simulated results we do calculate on the poly-dispersity frozen ferrofluids. That is, the poly-dispersity will decide the competition of magnetic phases (blocking or super-paramagnetic state) of dilute sample at the finite temperature.

First, we consider the temperature dependence of coercivity to show the suitable finite temperature in the current model. Fig. 5a shows the temperature dependence of coercivity. As the temperature is very low, the coercive decreases along with the dipolar interacting strength and with rising the temperature, the coercive field slower decay at the higher concentration. These results also were performed by Kechrakos & Trohidou (Kechrakos & Trohidou, 1998) in the mono-dispersity system. As a result, at a finite temperature, the coercive field increases along with the concentration and we may call this temperature as

the transition temperature which separates the anti-ferromagnetic and ferromagnetic regime. It is worth that the transition temperature is not unique, it depends on the change of concentration. This unique behavior leads to a difficulty for determining the magnetic phase diagram of ferrofluid viz. at a same temperature, a sample can be in the anti-ferromagnetic states in comparison with any sample having the lower concentration but in the ferromagnetic regime with the another one having the higher concentration. It is interesting that in a sample, the transition temperature is always less than the peak temperature of the dc zero-field-cooling magnetization curve. This result was also experimentally found in the strong interacting particle system (For example, Kleemann et al, 2001; Parker et al., 2008).
Fig. 5b performs magnetic coercivity vs. concentration curves at the finite temperature, T = 50 K (the dash line in Fig. 5a). The non-monotonousness expresses clearly in the mono-dispersity sample and the plateau-like shape appears with increasing the distribution width. If we continue raising the distribution width, the curves may monotonously decrease. As presented in the above result (sec. 4.1), with our system the blocking temperature of the mono-dispersity and weak interacting sample is about 50 K. Therefore, at the low concentration, the mono-dispersity sample has many super-paramagnetic particles, so as explained above the dipolar interaction deduces the increase of the magnetic response. On the contrary, in the strong poly-dispersity sample, the number of super-paramagnetic particles is small, therefore this weakens the non-monotonousness. With increasing the concentration, certainly, the dipolar interaction restores the demagnetizing role and then the coercivity decreases. Interestingly, magnetic responses at the low concentration completely separate, while they are close together at the high concentration. This situation again asserts the role exchange of the poly-dispersity and the dipolar interaction as discussed above. Clearly, the poly-dispersity also contributes to the complexity of the magnetic phase diagram of the magnetic nanoparticle system.

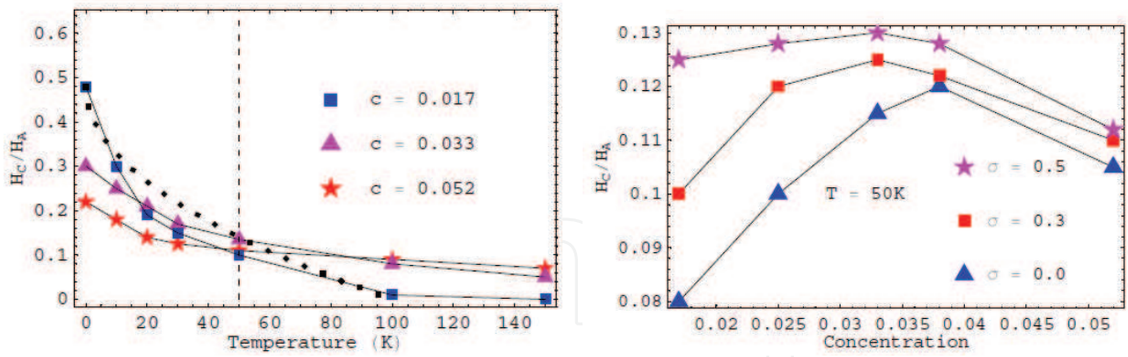

(a) (b)

Fig. 5. (a) Temperature dependence of coercive field as a function of concentration and (b) concentration dependence of the coercive field as a function of distribution width σ at the finite temperature T = 50 K (from Lan and Hai 2010)

4.3 Effective anisotropy in interacting assemblies at the finite temperature

As saw above, at a finite temperature, the dipolar interaction causes the enhancement of energy barrier which makes the coercive field increase. A question in here is what deduces this behavior? We attribute above behaviors to the thermal fluctuation of particle moments.

In the blocking state, under the influence of the anti-ferromagnetic character of dipolar interaction (the second term in Eq. 13) magnetic moments will tend to anti-parallel behaviors to minimize the dipolar energy. However, with increasing the temperature, the thermal fluctuation makes the random orientation of particle moments, and the anti-ferromagnetic role of the second term in Eq. 13 seems to be vanished. While the position of the particle does not change, in the other word, the bond axes are conserved. This leads to the dominance of the anisotropic component along the bond axes in the dipolar interaction (the second term in the Eq. 14), therefore the effective anisotropy increases. These arguments are proved by moment snapshots in Fig. 6. Positions of particles are chosen randomly. Configurations are recorded after the temperature is slowly enhanced from zero to 100 K. As we see in Fig. 6, the particle moments tend to the alignment along the bond axes in the direction of external field **H.**

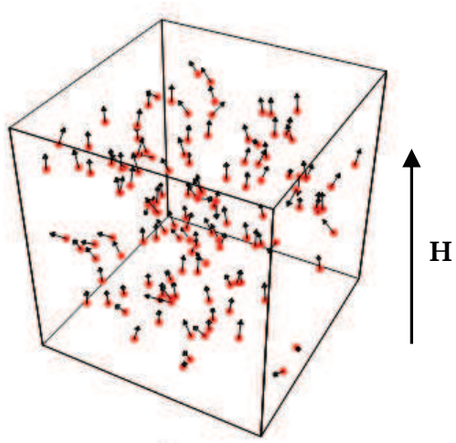

Fig. 6. Snapshot of 128 magnetic moment at the temperature T = 50 K, small arrows represent magnetic moments and the large solid arrow indicates the direction of external field

At each the given condition, the sample is firstly submitted to equilibrium state through 5.10^4 Monte Carlo steps. Next, we calculate the energy barrier (EB) and the effective anisotropy (EA) of each particle. (i) EB is determined similarly to the energy difference in each Monte Carlo step, but the only positive value is accepted. (ii) EA is calculated from Eq. 15. As we mentioned, although the effect of the external field was not clearly included in Eq. 15, it is implicated in the direction of magnetic moments.

Recent experimental results (Georgescu et al., 2006) in the two-dimension particle array of γ-Fe_2O_3 particles showed that dipolar interaction deduces flux closure configurations along the bond axes which blocks magnetic moments. As we introduced, the effective anisotropy (EA) was determined by the uniaxial anisotropy and anisotropic character along the bond axes of dipolar interaction, so we do compare between the EB distribution and the EA distribution with the change of the particle number at the T = 100 K as in Fig. 7. The uniaxial anisotropy constant is invariable, K_u = 19 kJ.m^{-3}. With the dilute sample, Fig. 7a, N = 64, the large-energy tails of the EA distribution and the EB distribution are strongly different, while the relative identicalness exists in the dense sample, N = 128, as in Fig. 7b. These lead to the assertion that the dipolar interaction dominates in the large-energy tails at the high-temperature as found in the experiment (Georgescu et al., 2006). In the later work, Georgescu et al. (Georgescu et al., 2008) showed that the role enhancing the energy barrier

of dipolar interaction strongly depends on temperature. This means that at the low temperature, the magnetic moments are blocked by influence of the intrinsic anisotropy. On the contrary, as the temperature is high enough the role of the intrinsic anisotropy become weak and the dipolar interaction dominate in the effective anisotropy which enhancing the blocking temperature. These results seem to respond to our argument in the section 4.2 about magnetic phase of interacting assemblies.

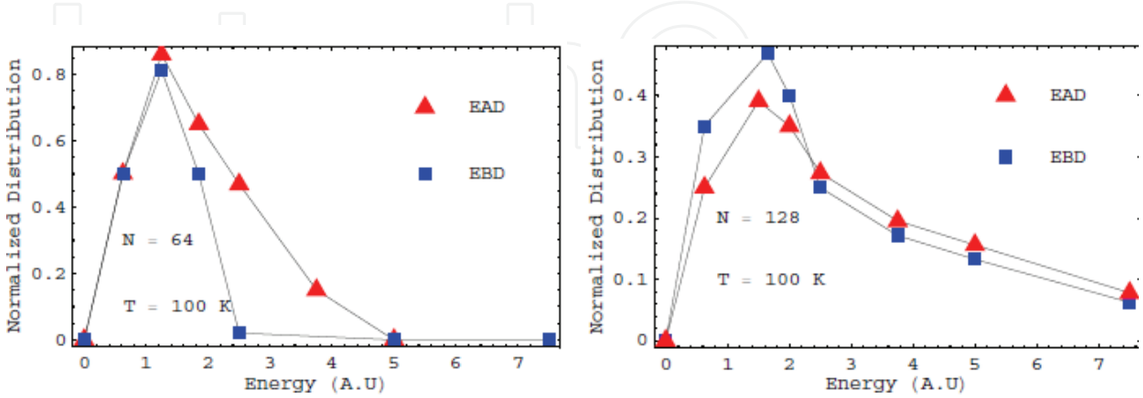

(a) (b)

Fig. 7. Comparison between the effective anisotropy distribution (EAD) and the energy barrier distribution (EBD) at finite temperature T = 100 K with the change of number of particles.

Finally, to show the effect of thermal fluctuation on the effective anisotropy deduced by the dipolar interaction, we perform the temperature dependence of the EA distribution as in Fig. 8. We can see that the distribution enlarges as the temperature increases. However, if the temperature is very high, the distribution becomes narrow. These can be explained as follow. At the low-temperature, magnetic moments have the anti-paralleling tendency to minimize the dipolar interacting energy. The effective anisotropy along the bond axis is therefore trivial. At the moderate temperature, the thermal fluctuation is small enough for weakness of the anti-ferromagnetic character of dipolar interaction and then the ferromagnetic character along the bond axis becomes important. However, at the very high temperature the strong thermal fluctuation makes the ferromagnetism disappearing.

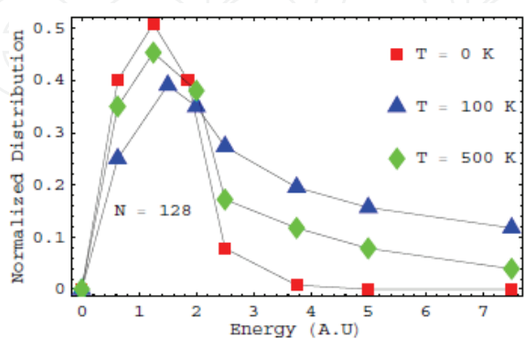

Fig. 8. Effective anisotropy distribution as a function of temperature

If temperature is continued increasing the sample behaves the paramagnetic character. These mean that EA distribution just has prime significance in a certain interval which is

around blocking temperatures. At very high temperature, the sample behaves the paramagnetic states. In the summary, the role of dipolar interaction strongly depends on the range of temperature.

5. Conclusions and future aspects

We presented several fundamental properties of frozen ferrofluids, which have not been sufficiently given by the phenomenal models, through the Monte Carlo simulation. These results are good conformity with found experiments.

- The field dependence of the blocking temperature behaves differences in the samples with the various concentrations. (i) The non-monotonousness in the dilute sample, which contrasts with the Neel - Brown theory, is due to the responses between the energy barrier distribution and the size distribution. These results showed effect of poly-dispersity on the blocking temperature in magnetic nanoparticle assemblies as found in the experiments. However, to clearly understand this non-monotonousness we may base on the recent results on the surface anisotropy of magnetic nanoparticles. (ii) The invariance of the blocking temperature along with the low-field in the dense sample is due to the role enhancing the anisotropy of the dipolar interaction. In other words, the dipolar interaction makes a new order sate which behaves the ferromagnetism along the bond axes.
- The demagnetizing role of the dipolar interaction strongly depends on the temperature as well as the poly-dispersity. We had proven that the main cause of the increase of coercivity along with the low concentration is due to the competition between the number of blocked and super-paramagnetic particles through the poly-dispersity, therefore, we believe that only the dipolar interaction has significance in the non-monotonous variation of the coercive field vs. concentration curve. We can see that the magnetic phase diagram of frozen ferrofluid not only depends on the concentration but also is affected by the poly-dispersity. At a finite temperature, the strong poly-dispersity retains the anti-ferromagnetic role of the dipolar interaction and the contrary, this role weakly expose in mono-dispersity samples. Finally, depending on the type of materials, the cusp can occur even at the room temperature, so we can control the concentration or the poly-dispersity of the sample in the preparation to satisfy applicable potentials.
- We have clearly explained the cause of the collective state at the high-temperature in frozen ferrofluid through the effective anisotropy distribution: at a temperature being near the blocking temperature, the thermal fluctuation deduces the vanishing of effect of the magneto-crystal anisotropy, while the collective dipole-dipole interaction enhances the effective anisotropy by forming the flux closure configurations along bond axes. In addition, our results also showed that the anisotropic character along the bond axis of dipolar interaction plays dominant role in effective anisotropy at the interval of temperature being near blocking temperature. We can apply this relatively simple way to explain the collective sates in the systems of different spatial arrangement

In our opinions, there are some suggestions on the theoretical model on magnetic properties and the simulations in biomedical applications as follow

- As we discussed above, there are two ways to include the dipolar interaction on the other terms, namely applied field and the uniaxial anisotropy. Therefore, depending on the range of temperature (low- or high-temperature), we select the suitable model. For

example, at the low temperature, we can develop mean field theory to describe the super-spin glass behaviors or at the high temperature, we can use the model of Dormann et al. 1988 to show the ferromagnetic states of the interacting assemblies, however with more exactly parameter. Clearly that no model can cover all complexities of interacting magnetic nanoparticle assemblies, so each model just describe properties of assemblies in the specific case.

- Recent simulated as well experimental studies on applications of collective particles in biomedicine (Schaller et al., 2009; Dennis et al., 2007, 2008) showed great promises. Therefore, we need to develop computer simulations to optimize as well as predict the applicable potentials of the collective state at the high temperature, such as effect of interactions on heating in hyperthermia, resonance of magnetic moment in contrast agents, the transport in drug delivery or cell separation. Besides, the collective particle assemblies may open new applications which we have to very much effort to find.

6. References

Allia, P.; Coisson, M.; Tiberto, P.; Vinai, F.; Knobel, M.; Novak, M. A. & Nunes, W. C. Granular Cu-Co alloys as interacting superparamagnets. *Phys. Rev. B,* Vol. 64, (September, 2001), pp. 144420 (1-12), ISSN: 1098-0121

Andersson, J.-O.; Djurberg, C.; Jonsson, T.; Svedlindh, P. & Nordblad, P. (1997). Monte Carlo studies of the dynamics of an interacting monodispersive magnetic-particle system. *Phys. Rev. B*, Vol. 56 (December, 1997), pp. 13983-13988, ISSN: 1098-0121

Azeggagh, M. & Kachkachi, H. (2007). Effects of dipolar interactions on the zero-field-cooled magnetization of a nanoparticle assembly,*Phys. Rev. B*, Vol. 75 (May, 2007), pp. 174410 (1-9), ISSN: 1098-0121

Blackwel,l J. J.; Morales, M.P.; O'Grady,K.; Gonzalez, J.M.; Cebollada,F.& Alonso-Sanudo, M.(2003), Interactions and hysteresis behaviour of Fe/SiO_2 Nanocomposites, *J. Mag. Mag. Mat.,*Vol. 242-245 (2003), pp. 1103-1105, ISSN: 0304-8853.

Bottoni, G.; Candolfo, D.; Cecchetti, M.; Corradi, A. R. & Masoli, F. (1993). Influence of packing density on the coercivity of iron particles for magnetic recording, *J. Mag. Mag. Mat*., Vol. 120 (1993), pp. 167-171, ISSN: 0304-8853.

Brown, W. F. Jr. (1963). Thermal Fluctuations of a Single-Domain Particle. *Phys. Rev.*, Vol.130 (June, 1963), pp. 1677-1686. ISSN: 0031-9007.

Ceylan, A.; Bakker, C. C.; Hasanain, S. K. & Shah S. I. (2005). Nonmonotonic concentration dependence of magnetic response in Fe nanoparticle-polymer composites, *Phys. Rev. B,* Vol. 72, (October, 2005), pp. 134411, ISSN: 1098-0121

Dennis, C. L.; Jackson, A. J.; Borchers, J. A.; Ivkov, R.; Foreman, A. R.; Lau, J. W.; Goernitz, E. & Gruettner, C. (2008). The influence of collective behavior on the magnetic and heating properties of iron oxide nanoparticles, *J. Appl. Phys.*, Vol. 103, (March, 2008), pp. 07A319 (1-3), ISSN: 0021-8979.

Dormann, J. L ; Fiorani, D. & Tronc, E. (1999). On the models for interparticle interactions in nanoparticle assemblies: comparison with experimental results, *J. Mag. Mag. Mat.*, Vol. 202, (1999), 251-267, ISSN: 0304-8853.

Fernández, J. F. & Alonso. J. J. (2009). Equilibrium spin-glass transition of magnetic dipoles with random anisotropy axes on a site-diluted lattice, *Phys. Rev. B*, Vol. 79, (June, 2009) 214424 (1-6), ISSN: 1098-0121.

Friedman, J. R., Voskoboynik, U. & Sarachik, M. P. (1997). Anomolous magnetic relaxation in ferritin, *Phys. Rev. B*, Vol. 56 (November, 1997) pp. 56 10793, ISSN: 1098-0121.

Garcia-Otero, J.; Porto, M; Rivas, J. & Bunde, A. (2000). Influence of magnetic properties of ultra-fine ferromagnetic particles, *Phys. Rev. Lett.*, Vol. 84 (January, 2000), pp. 167-170, ISSN: 0031-9007.

Georgescu, M.; Viota, J. L; Klokkenburg, M.; Erné, B. H.; Vanmaekelbergh, D. & Zeijlmans van Emmichoven, P. A. (2006). Flux closure in two-dimensional magnetite nanoparticle assemblies, *Phys. Rev. B*, Vol. 73 (May, 2006), pp. 184415 (1-5), ISSN: 1098-0121.

Georgescu, M.; Viota, J. L; Klokkenburg, M.; Erné, B. H.; Vanmaekelbergh, D. & Zeijlmans van Emmichoven, P. A. (2008) Short-range magnetic order in two-dimensional cobalt-ferrite nanoparticle assemblies, *Phys. Rev. B*, Vol. 77 (January, 2008), pp. 024423 (1-6), ISSN: 1098-0121.

Iglesias, O. & Labarta, A. (2004). Magnetic relaxation in terms of microscopic energy barriers in a model of dipolar interacting nanoparticles, *Phys. Rev. B*, Vol. 70, (February, 2004), 144401, ISSN: 1098-0121.

Jonsson, T.; Mattsson, J.; Djurberg, C.; Khan, F. A.; Nordblad, P. & Svedlindh, P. (1995). Aging in a magnetic nanoparticle systems, *Phys. Rev. Lett.*, Vol. 75, (November, 1995), 4138, ISSN: 0031-9007.

Kackachi, H.; Coffey, W. T.; Crothers, D. S. F.; Ezzir, A.; Kenedy, E. C.; Nogues, M. & Trone, E. (2000). Field dependence of the temperature at the peak of the zero-field-cooled magnetization. *J. Phys.: Condens. Matter*, Vol. 12, (November, 2000), pp. 3077, ISSN: 0953-8984.

Kechrakos, D. & Trohidou, K. N. (1998). Magnetic properties of dipolar interacting single-domain particles, *Phys. Rev. B*, Vol. 58 (November, 1998), pp. 12169, ISSN: 1098-0121.

Kechrakos, D. (2010). Magnetic nanoparticle assemblies. *Pre-print* (April, 2010).

Kleemann, W.; Petracic, O.; Binek, Ch.; Kakazei, G. N.; Pogorelov, Y. G.; Sousa, J. B.; Cardoso, S. & Freitas, P. P. (2001). Interacting ferromagnetic nanoparticles in discontinuous $Co_{80}Fe_{20}$ /Al_2O_3 multilayers: From superspin glass to reentrant superferromagnetism. *Phys. Rev. B*, Vol. 63 (March, 2001), pp. 134423 (1-5), ISSN: 1098-0121.

Knobel, M.; Nunes, W. C.; Socolovsky, L. M.; De Biasi, E.; Vargas, J. M. & Denardin, J. D. (2008). Superparamagnetism and other magnetic features in granular materials: A Review on Ideal and Real Systems, *J. Nanosci. Nanotech.*, Vol. 8 (2008), pp. 2836-2857, ISSN: 1550-7041.

Lan, T. N. & Hai, T. H (2010). Monte Carlo simulation of magnetic nanoparticle systems. *Comput. Mater. Sci.*, Vol. 49 (March, 2010), pp. S287-S290, ISSN: 0927-0256.

Lan, T. N. & Hai, T. H. (2010). Role of poly-dispersity and dipolar interaction in magnetic nanoparticle systems: Monte Carlo study. *J. Non-Cryst. Solids*. in press (December, 2010). ISSN: 0022 - 3093

Luo, W.; Nagel, S. R.; Rosenbaum, T. F. & Rosensweig, R. E. (1991). Dipole interactions with random anisotropy in a frozen ferrofluid, *Phys. Rev. Lett.*, Vol. 67, (November, 1991), 2721, ISSN: 0031-9007.

Malik, R.; Lamba, S.; Kotnala, R.K. & Annapoorni1, S. (2010). Role of anisotropy and interactions in magnetic nanoparticle systems. *Eur. Phys. J. B*, Vol. 74, (February, 2010), pp. 75-80, ISSN: 1434-6028.

Metropolis, N.; Rosenbluth, A. W.; Rosenbluth, M. N.; Teller, A. H. & Teller, E. Equation of State Calculations by Fast Computing Machines. *J. Chem . Phys.*, Vol. 21 (March, 1953), pp. 1699114 (1-6), ISSN: 0021-9606.

Morup, S. & Tronc, E. (1994). Superparamgnetic relaxation of weakly interacting particles, *Phys. Rev. Lett.*, Vol. 72 (May, 1994), pp. 3278-3281, ISSN: 0031-9007.

Neel, L. (1953). Thermoremanent magnetization of fine powders. *Rev. Mod. Phys.*, Vol. 25 (1953), pp. 293-295, ISSN: 0034-6861.

Nunes, W. C.; Socolovsky, L. M.; Denardin, J.C.; Cebollada, F.; Brandl, A. L & Knobel, M. Role of magnetic interparticle coupling on the field dependence of the superparamagnetic relaxation time, *Phys. Rev. B*, Vol. 72 (December, 2005), pp. 212413 (1-4), ISSN: 1098-0121.

Pankhurst, Q. A.; Connolloy, J.; Jones, S .& Dobson, J. (2003). Applications of magnetic nanoparticles in biomedicine. *J. Phys. D: Appl. Phys.*, Vol. 36 (June, 2003), pp. R167 - R181, ISSN: 0022-3727.

Parker, D.; Dupuis, V.; Ladieu, F.; Bouchaud, J.-P.; Dubois, E.; Perzynski, R. & Vincent, E. (2008), Spin glass behavior in an interacting γ-Fe_2O_3 nanoparticle system, *Phys. Rev. B*, Vol. 77 (March, 2008), 104428(1-9), ISSN: 1098-0121.

Perez, N.; Guardia, P.; Roca, A. G.; Morales, M. P.; Serna, C. J.; Iglesias, O.; Bartolomé, F.; García, L. M.; Batlle, X. & Labarta, A. (2008) Surface anisotropy broadening of the energy barrier distribution in magnetic nanoparticles, *Nanotechnology*, Vol. 19, (October, 2008), pp. 475704, ISSN: 0957-4484.

Porto., M. (2005). Ordered systems of ultrafine ferromagnetic particles, *Eur. Phys. J. B*, Vol. 45 (January, 2005), pp. 369-375, ISSN: 1434-6028.

Prokopieva, T. A.; Danilov, V. A.; Kantorovich, S. S. & Holm, C. (2009). Ground state structures in ferrofluid monolayers, *Phys. Rev. B*, Vol. 80 (September, 2009), pp. 031404 (1-13), ISSN: 1098-0121.

Sappey, R.; Vincent, E.; Hadacek, N.; Chaput, F.; Boilot, J. P. & Zins, D. (1997). Nonmonotonic field dependence of the zero-field cooled magnetization peak in some systems of magnetic nanoparticles, *Phys. Rev. B*, Vol. 56 (December, 1997), 14551, ISSN: 1098-0121.

Schaller, V; Wahnström, G.; Sanz-Velasco, A.; Gustafsson, S.; Olsson, E.; Enoksson, & Johansson, C. (2009). Effective magnetic moment of magnetic multicore nanoparticles *Phys. Rev. B.*, Vol. 80 (September, 2009), 092406, ISSN: 1098-0121.

Serantes, D.; Baldomir, D., Pereiro, M., Arias, J.E.; Mateo-Mateo, C.; Bujan-Nunez, M.C.; Vazquez-Vazquez, C. & Rivas, J. (2008). Interplay between the magnetic field and the dipolar interaction on a magnetic nanoparticle system: A Monte Carlo study, *J. Non Crystalline Solids*, Vol. 354, (October, 2008), pp. 5224-5226, ISSN: 0022-3093.

Tamion, A.; Raufast, C.; Hillenkamp, M.; Bonet, E.; Jouanguy, J.; Canut, B.; Bernstein, E.; Boisron, O.; Wernsdorfer, W. & Dupuis, V. (2010). Magnetic anisotropy of embedded Co nanoparticles: Influence of the surrounding matrix. *Phys. Rev. B*, Vol. 81 (April, 2010), pp. 144403 (1-6), ISSN: 1098-0121.

Tan, R. P.; Lee, J. S.; Cho, J. U.; Noh, S. J; Kim, D. K. & Kim, Y. K. Numerical simulations of collective magnetic properties and magnetoresistance in 2D ferromagnetic nanoparticle arrays, *J. Phys. D: Appl. Phys.*, Vol. 43, (March, 2010), pp. 165002 (1-8), ISSN: 0022-3727.

Ulrich, M.; Garcıa-Otero, J.; Rivas, J. & Bunde, A. (2003). Slow relaxation in ferromagnetic nanoparticles: Indication of spin-glass behavior, *Phys. Rev. B* Vol. 67 (January, 2003) 026616 (1-4), ISSN: 1098-0121.

Verdes, C.; Ruiz-Diaz, B.; Thompson, S. M.; Chantrell, R. W. & Stancu, Al. (2002). Computational model of the magnetic and transport properties of interacting fine particles. *Phys. Rev. B* Vol. 65, (April, 2002), pp. 174417 (1-10), ISSN: 1098-0121.

Walton, D. (2006). A theory for spin glass phenomena in interacting nanoparticle systems. *Pre-print*, (August, 2006).

Yang, Y.; Shen, S.; Ye, Q.; Lin, L. & Huang, Z. (2006). The roles of the exchange and dipole couplings on the magneto-resistance for the nanoparticle arrays, *J. Mag. Mag. Mat.*, Vol. 303, (March, 2006), pp. e312-e314, ISSN: 0304-8853.

Zheng, R. K; Gu, H.; Xu, B. & Zhang, X. X. (2006). The origin of the non-monotonic field dependence of the blocking temperature in magnetic nanoparticles. *J. Phys.: Condens. Matter*, Vol. 18, (June, 2006), pp. 5905, ISSN: 0953-8984.

Zheng, R. K.; Gu, H.; Zhang, B.; Liu, H.; Zhang, X. X. & Ringer, S. P. (2009). Extracting anisotropy energy barrier distributions of nanomagnetic systems from magnetization/susceptibility measurements. *J. Mag. Mag. Mat.,* Vol. 312 (2009), pp. L21-L27, ISSN: 0304-8853

Applications of Monte Carlo Method in Science and Engineering
Edited by Prof. Shaul Mordechai

ISBN 978-953-307-691-1
Hard cover, 950 pages
Publisher InTech
Published online 28, February, 2011
Published in print edition February, 2011

In this book, Applications of Monte Carlo Method in Science and Engineering, we further expose the broad range of applications of Monte Carlo simulation in the fields of Quantum Physics, Statistical Physics, Reliability, Medical Physics, Polycrystalline Materials, Ising Model, Chemistry, Agriculture, Food Processing, X-ray Imaging, Electron Dynamics in Doped Semiconductors, Metallurgy, Remote Sensing and much more diverse topics. The book chapters included in this volume clearly reflect the current scientific importance of Monte Carlo techniques in various fields of research.

InTech Europe
University Campus STeP Ri
Slavka Krautzeka 83/A
51000 Rijeka, Croatia
Phone: +385 (51) 770 447
Fax: +385 (51) 686 166
www.intechopen.com

InTech China
Unit 405, Office Block, Hotel Equatorial Shanghai
No.65, Yan An Road (West), Shanghai, 200040, China
中国上海市延安西路65号上海国际贵都大饭店办公楼405单元
Phone: +86-21-62489820
Fax: +86-21-62489821

IntechOpen